Article:

Lal, S, Hall, RM and Tipper, JL orcid.org/0000-0002-8719-0323 (2016) A Novel Method for Isolation and Recovery of Ceramic Nanoparticles and Metal Wear Debris from Serum Lubricants at Ultra-low Wear Rates. Acta Biomaterialia, 42. pp. 420-428. ISSN 1742-7061

https://doi.org/10.1016/j.actbio.2016.07.004

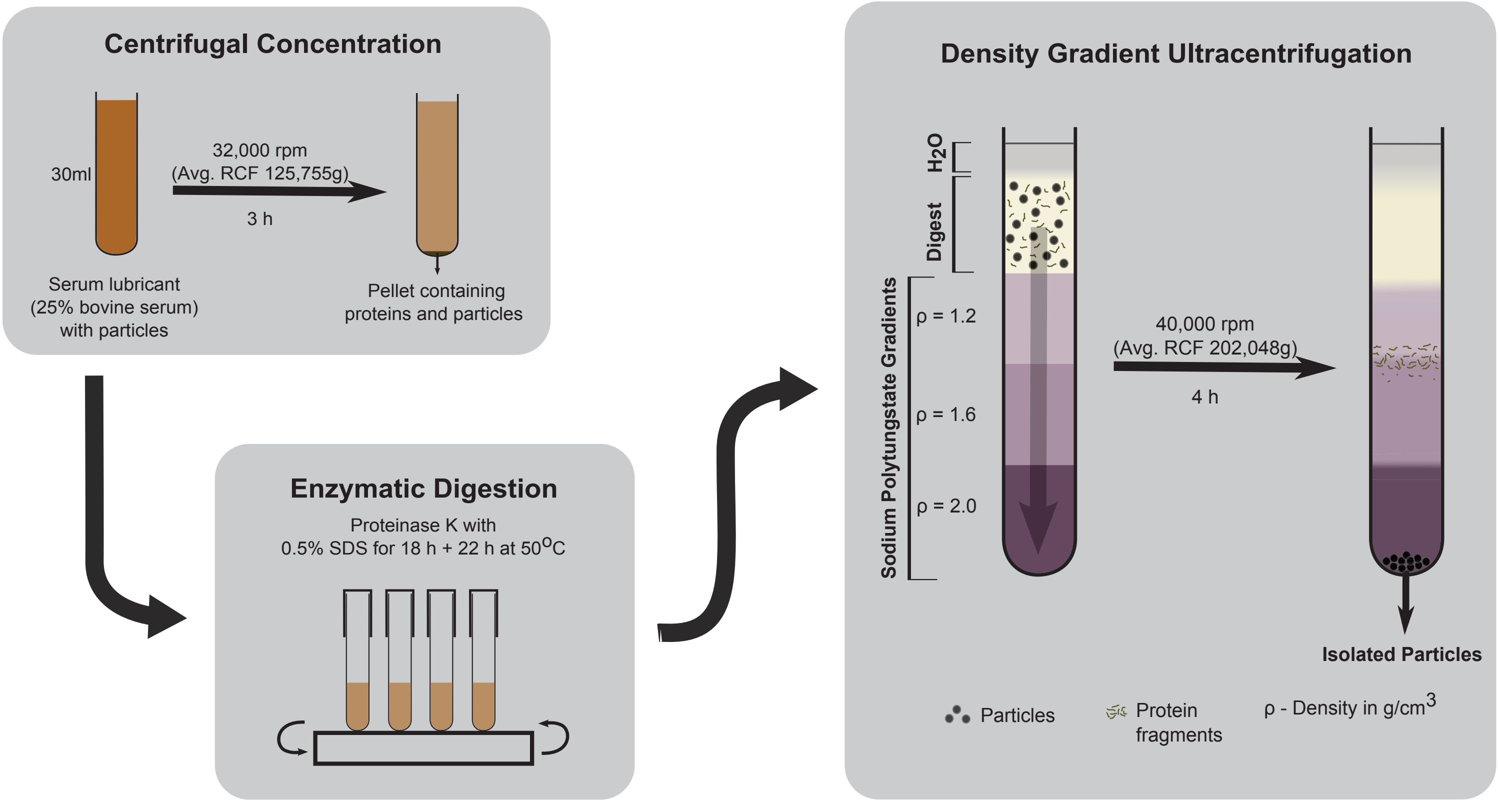

Figure 1 A scheme for the particle isolation procedure. The method is divided into concentration, enzymatic digestion and isolation steps.

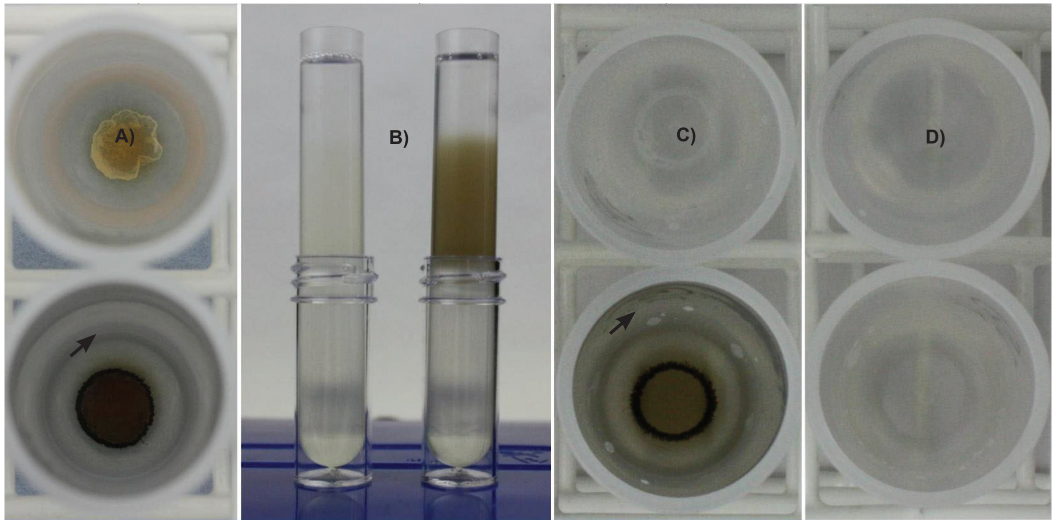

Figure 2 Isolation of Si3N4 and CoCr particles from 25% (v/v) bovine serum lubricant. A) Si3N4 (top) and CoCr (bottom) lubricant samples pelleted after concentration step as indicated by arrows. Pellets appear yellowish due to the presence of protein contaminants. B) Sodium polytungstate gradients prior to centrifugation (Left: Si3N4, Right: CoCr). C) Si3N4 (top) and CoCr (bottom) particles pelleted at the end of centrifugal washing as indicated by arrows. The colour of the digested lubricant layer in the right tube was darker due to the presence of CoCr particles. D) Si3N4 (top) particles doped at ultra-low wear rates were not visible to the naked eye after washing steps. CoCr (bottom) particles doped at ultra-low wear rates were hardly visible to the naked eye after washing steps as indicated by the arrow.

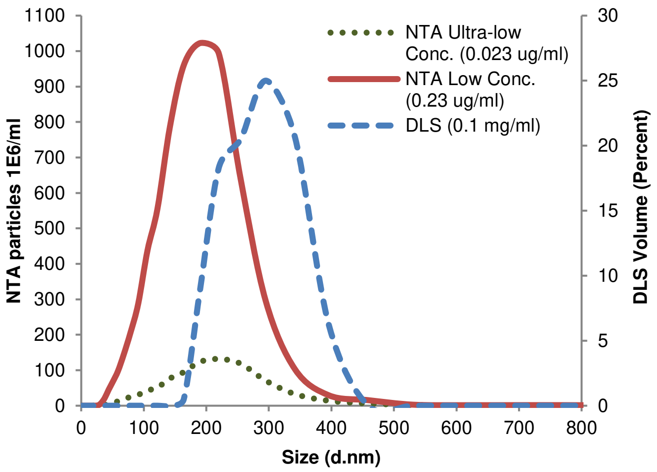

Figure 3 Size distribution from NTA measurements of Si3N4 nanoparticles dispersed in water at ultra-low concentration (dotted line) and low concentration (solid line). Size distribution from DLS measurements of 0.1 mg.ml-1 Si_3N_4 nanoparticles (dashed line). Maximum aggregate size for Si_3N_4 nanoparticles was approximately 500 nm with both NTA and DLS measurements.

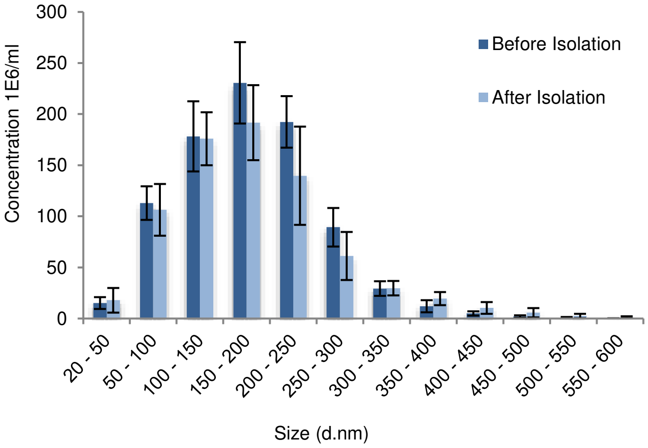

Figure 4 Particle size distribution of Si3N4 aggregates before and after the particle isolation procedure measured by NanoSight at ultra-low wear rates of 0.01mm3/million cycles. The size distribution of aggregates remained unaffected by the method. Error bars show standard deviation. No significant differences were observed in particle size before and after isolation (Kolmogorov-Smirnov Z test, P>0.05).

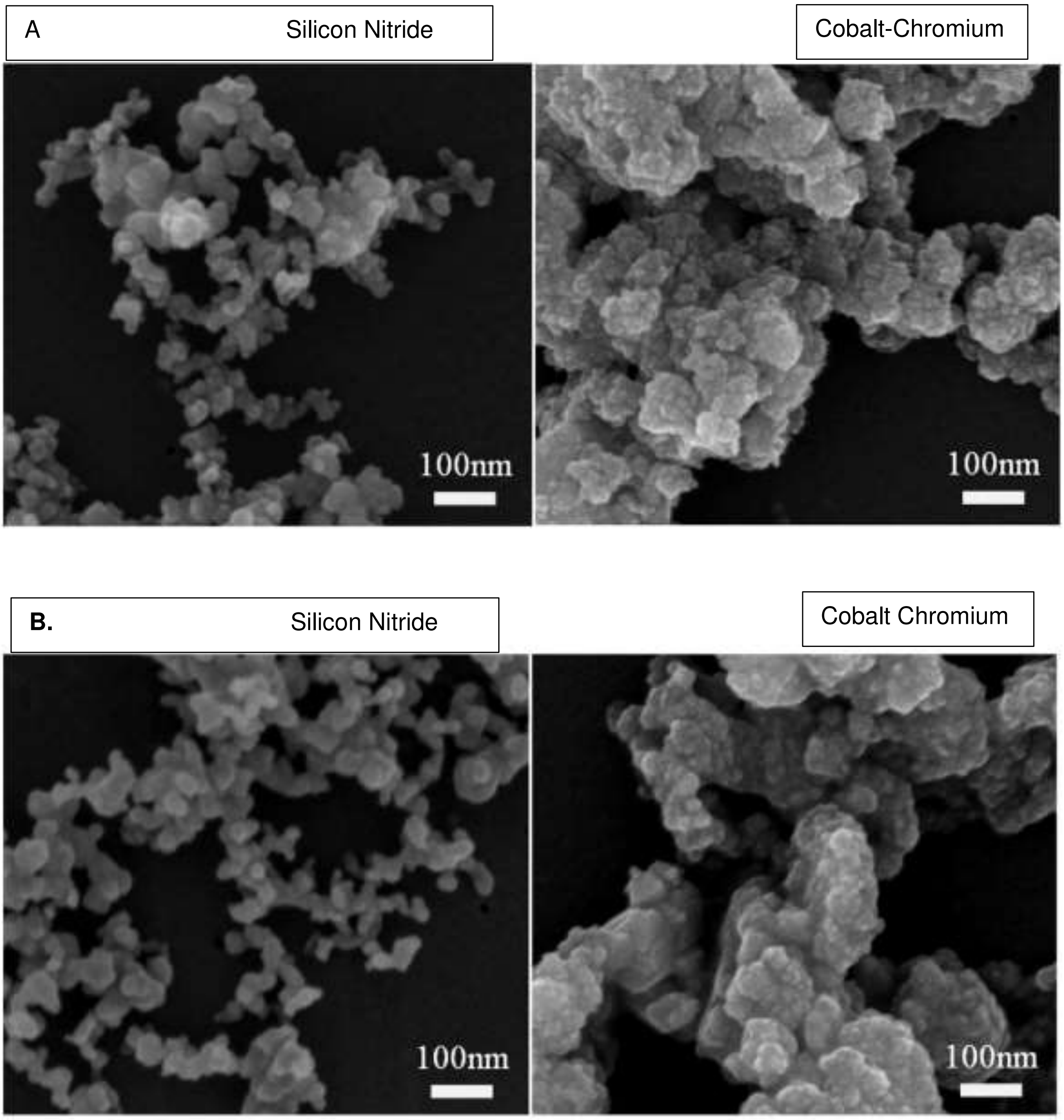

Figure 5 Scanning electron micrographs of Si3N4 and CoCr particles. A) Before the isolation procedure. B) After the isolation procedure. The morphology of particles was similar in both cases indicating no noticeable effect of the novel isolation method on the particles.

A)

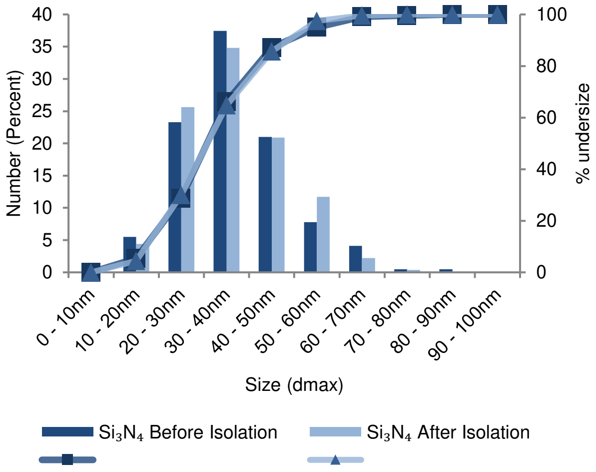

B)

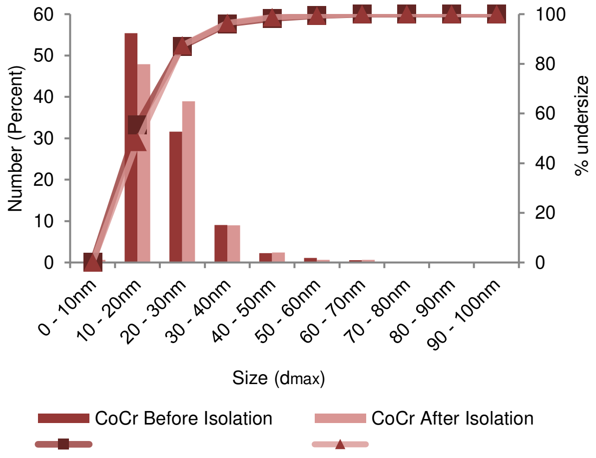

Figure 6 A comparison of particle size distributions of primary particles before and after the isolation procedure. A) Si3N4 50nm model particles. B) CoCr wear debris. Particle size distributions before and after isolation were not significantly different (Kolmogorov-Smirnov Z test, P>0.05).

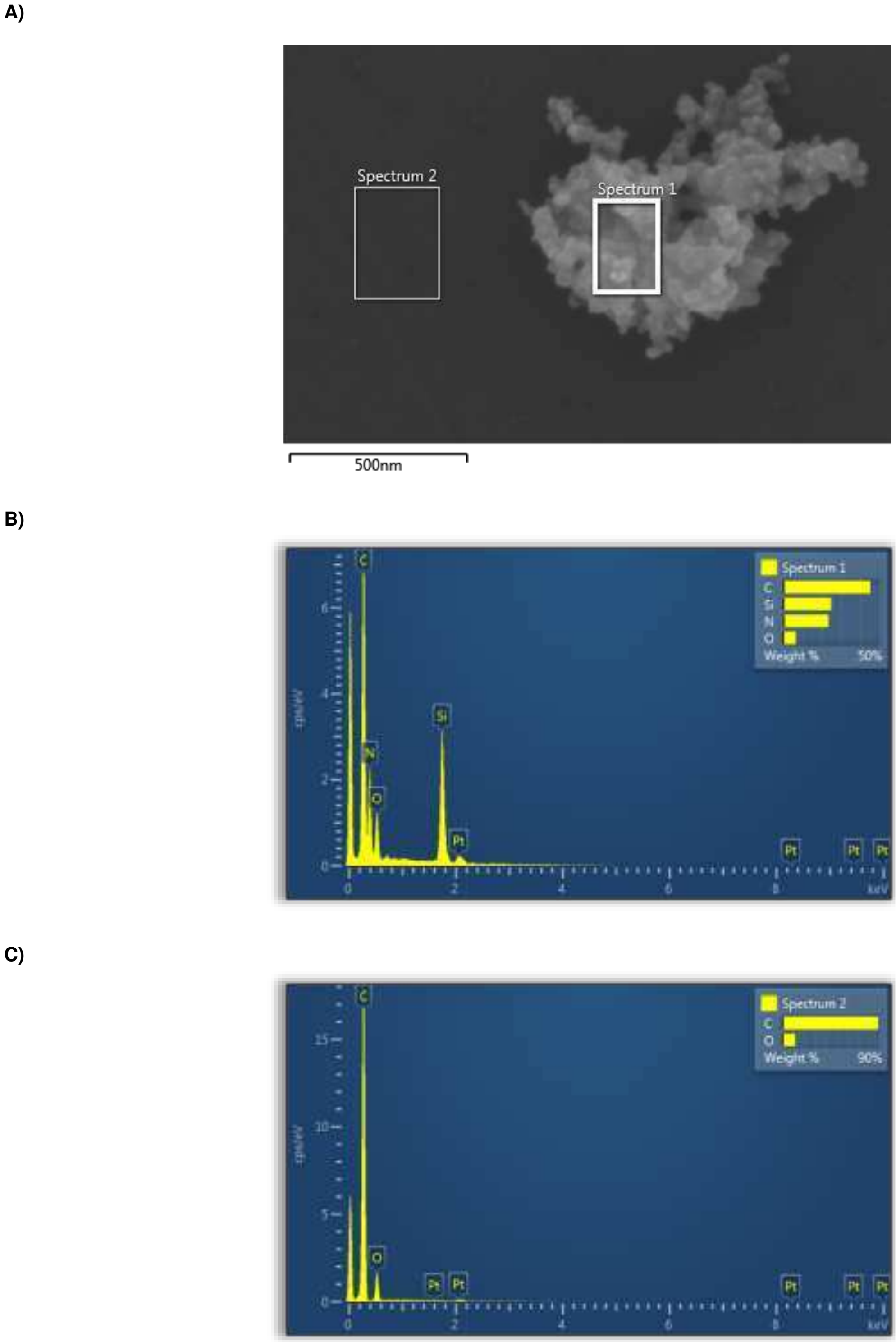

Figure 7 Energy-dispersive X-ray analysis of Si3N4 particles collected on 0.015 µm Nucleopore membrane filters. High spatial resolution (less than 300 nm) was achieved by using a large area SDD detector (80 mm2 X-Max SDD, Oxford Instruments) and an accelerating voltage of 5 kV. A) Particle (spectrum 1) and background areas (spectrum 2) used for EDX analysis. B) EDS spectrum of Si3N4 particles showing silicon, nitrogen, carbon, oxygen and platinum peaks. C) EDS spectrum of background filter showing carbon, oxygen and platinum peaks. Membrane filters were composed of polycarbonate polymer and therefore showed carbon and oxygen peaks for both areas. Platinum peaks were due to the platinum coating applied to all samples.

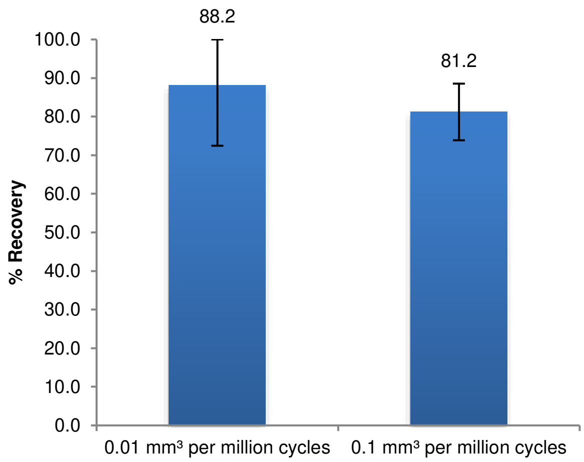

Figure 8 Percentage recovery of Si3N4 nanoparticles from 25% (v/v) NCS lubricant at ultra-low wear rates of 0.01 mm3 per million cycles and low wear rates of 0.1 mm3 per million cycles using the novel method. Error bars show standard deviation.